AUT Journal of Mechanical Engineering

AUT J. Mech. Eng., 4(4) (2020) 553-564
DOI: 10.22060/ajme.2020.16132.5806

# Theoretical and Numerical Analysis of Jamming Phenomenon in Positioning of Circular Workpiece on Horizontal Surface

Hadi Parvaz*

Faculty of Mechanical and Mechatronics Engineering, Shahrood University of Technology, Shahrood, Iran

**ABSTRACT:** Grasping or positioning workpiece with circular geometry is a common process in fixture design and robotic manipulation systems. The typical two-contact mechanisms that are usually used for gripping or positioning of these kinds of workpieces are prone to jam. Determination of the conditions in which jamming occurs in such systems seems to be necessary for research purposes as well as industrial applications. In the present study, jamming of the workpiece with the circular cross-section is investigated during its positioning on the horizontal surface. The theoretical foundation is established based on two models as far as the force equilibrium equations and the minimum norm principle. Validation of the theoretical predictions is conducted through the numerical analysis in the Adams software. The distance that the workpiece should travel to jam is obtained from the numerical analysis and compared to the theoretical predictions. By assuming the coefficient of friction equal to 0.4 and the radius of the workpiece equal to 10mm, jamming-in travel of the workpiece was obtained as 24.38mm and 25.58mm from the theoretical models and numerical analysis, respectively. A relative error of 4.9% is obtained between the theoretical predictions and numerical results. This value indicates the accuracy of predictions of the suggested theoretical models and the credibility of their results.

**Review History:**

Received: Apr. 14, 2019
Revised: Dec. 17, 2019
Accepted: Jan. 26, 2020
Available Online: Feb. 04, 2020

**Keywords:**

Circular workpiece
Fixture design
Jamming analysis
Positioning
Robotic assembly

## 1. INTRODUCTION

Jamming is defined as the sudden and unwanted immobilization of the workpiece during its loading into the fixture or grasping in the manipulation tasks. Jamming is not exclusively occurred in the fixturing systems. It may also occur during object grasping or positioning in the robotic manipulation systems. Jamming occurrence in such systems may cause severe damage to the workpiece, fixture elements, and robotic elements of the grasping systems. So, development of the robust and reliable models seems to be necessary for the prediction of jamming occurrence in these systems. Workpiece geometry plays an important role in the analysis of the jamming phenomenon. Block and palm case study has been extensively used for evaluating the capabilities of the previously-developed theoretical models. In this case study, workpiece geometry is of the polyhedral type which eases the grasping or positioning tasks. Circular workpieces are also used in industrial applications; both in fixturing applications and robotic manipulation systems. Such applications can be named as locating and positioning the workpiece with circular cross-sections using the V-type locators, positioning the cells in the robotic surgery systems, pick and place of the lenses using pence in eye surgery, etc. Despite these extensive applications, a gap is observable in the determination of the conditions in which jamming occurs in the manipulating or positioning of the workpieces with circular cross-sections. Fulfilling this research gap in the present study, jamming of the circular workpiece is investigated during its positioning on the horizontal surface by using a palm that is rotated around a fixed point. Theoretical and numerical approaches are used for this purpose. The proposed theoretical model may be used as a powerful tool for analyzing the stability of the workpiece with circular cross-section on the V-type locators. It should be mentioned that the optimum angle of the V-type locator which provides the best stability for the workpiece with circular cross-section depends on the materials of the workpiece and locators, coefficient of friction and intensity, and direction of the external wrenches. By considering these parameters, this angle can be calculated by using the suggested theoretical model. Also, the proposed configuration can be employed as a case study by further researchers to validate the predictions of their theoretical models.

## 2. LITERATURE SURVEY

Several types of research have been published for theoretical modeling of the jamming phenomenon in fixture design and robotic manipulation systems. Force analysis in quasi-static conditions, multi-body contact dynamics, and minimum norm principle have been used as the main tools for modeling the jamming phenomenon. In the first and second categories,

*Corresponding author's email: h.parvaz@shahroodut.ac.ir

contact mode (sliding or rolling) between the workpiece and fixturing (or positioning) elements are first determined by dynamic models, and based on that, jamming occurrence is predicted for the workpiece. In the third category, reaction forces at the contact points are first determined and jamming is predicted by the determination of the contact modes. Pang et al. [1] modeled the jamming problem as an uncoupled complementarity problem. By assuming that all contacts were initially in rolling mode, velocity and acceleration parameters were measured at the contact points. The problem was solved by the assumption of the non-linear Coulomb's friction model at the contact points. It was also shown that there always exists a solution for the multi-rigid-body problem with contacts in the initial rolling modes. Dupont and Yamajako [2] classified the analysis of the frictional multi-rigid-body contact problem into two categories, namely jamming and wedging phenomena. Wedging was defined as the special case of jamming at the static condition in which the reaction forces were linearly dependent at the contact points. Jamming was modeled by the development of a multi-body dynamics model and its occurrence was predicted based on the calculation of the contact velocity and acceleration values. In basic and comprehensive studies, Trinkle et al. [3, 4] studied the requirements of non-jamming conditions for the workpiece in the fixturing application. The analysis was performed in the quasi-static condition. Contacts were assumed to be in the initially sliding modes. It was predicted that jamming would occur for the workpiece by changing the contact condition at any of the contacts from sliding to the rolling modes. Two case studies were used for the evaluation of the capabilities of the proposed model in the prediction of jamming occurrence including peg-in-hole and block and palm problems. In the block and palm case study with the mentioned assumptions, it was concluded that the block started to jam at the distance of 0.75m. This result was used as the reference value in further papers for evaluating the proposed theoretical models. The proposed model investigated the jamming occurrence conditions in a quasi-static condition and it didn't take into account the effects of the inertia, kinematic and dynamic parameters of the block's motion. Balkcom and Trinkle [5] proposed a mathematical model for the determination of the external wrenches which were consistent with the predefined contact modes. The suggested model capabilities were evaluated through case studies in the fixture design application. Liu and Wang [6] used a time-stepping method for the calculation of the relative velocity and friction forces at the contact points between the rigid bodies. The rigid-body frictional contact problem was modeled based on the numerical approach and solved using the Gauss-Seidel iterative method. Results were compared to those of the uncoupled complementarity problem. In an attempt to predict jamming occurrence in the fixture design application, Liu et al. [7] suggested a mathematical model based on the rigid body contact problem under the application of the external wrenches. It was assumed that jamming would not occur if all of the contacts were in the sliding modes. The suggested model was evaluated through peg-in-hole and block and palm case studies. It was concluded that the external wrenches which kept all of the contact points in the sliding mode, maintain the whole system in the non-jamming condition. In the block and palm case study which was solved with the same assumptions used in the study of Trinkle et al. [4], it was concluded that the block started to jam at a distance equal to 0.25m. The proposed model took into account the effects of the dynamic parameters of the block's motion. Bender et al. [8] published a state-of-the-art paper to present and compare the software developments and mathematical algorithms that have been developed for interactive simulation of the rigid body contact problem. The mathematical foundations for modeling the rigid body contact problems were also reviewed such as complementarity problems, Newton-Euler equations, energy-based models as well as numerical methods. Simulation of the rigid body contact problem was conducted by Flickinger et al. [9] in an interactive environment. Several numerical methods were employed and their results were compared to each other. By comparing the polyhedral exact geometry method to the Stewart-Trinkle model, it was concluded that the former model required a smaller time step size to reach the accuracy of the latter one. In the study of Lu et al. [10], a benchmarking framework was developed to evaluate the efficiency of the solution methods that have been used for solving the multibody dynamics problems. In the proposed framework, complementarity problems were constructed for each simulation problem based on the initially provided data. Several solver options were provided in the benchmarking platform such as fixed-point iteration methods, non-smooth Newton method, Lemke's algorithm, etc. After benchmarking the solution methods, the most appropriate solution method was suggested for a 2D manipulation task. Parvaz and Nategh [11] proposed a mathematical model based on the minimum norm principle for the prediction of jamming occurrence for freeform workpieces at the fixture design application. By solving the optimization problem, the jamming occurrence was predicted between the workpiece and fixturing elements by application of the loading/unloading wrenches. Validation of the theoretical predictions was conducted by using three case studies: peg-in-hole, block and palm and a 3D workpiece with freeform surfaces. Recently, a theoretical model based on the minimum norm principle has been incorporated for prediction of workpiece jamming in the fixture design application. In the study of Parvaz and Nategh [12], minimum norm principle was used for avoiding jamming occurrence in the designing the locating system for parts with freeform surfaces. It was also employed in the study of Nategh and Parvaz [13] for checking the workpiece stability in the fixture by application of the clamping and weight-induced wrenches.

Recently, several types of research have been published on the investigation of jamming occurrence in dual peg-in-hole assembly systems. For this purpose, different methods of optimization and vision-guided or haptic systems have been incorporated by several researchers. In references [14, 15], a fuzzy-based model was proposed for the determination and control of contact forces and contact modes at both rigid and flexible dual peg-in-hole assembly systems. Experimental tests were also conducted to verify the effectiveness of the proposed force control and jamming prediction strategies. Huang et al. [16] suggested a grasping and positioning strategy for a specific two-hand robot to perform an automated intelligent peg-in-hole assembly process. By installing a vision system at the robot's end-effector and compensating the assembly error using the vision data, the proposed strategy was evaluated using the peg-in-hole assembly system with a clearance equal to 1mm. Hou et al. [17] proposed an impedance control strategy for modeling the robotic dual peg-in-hole assembly process as an optimization problem. The model was solved by an evolutionary algorithm combined with the support regression vector method for evaluation of the fitness values of the control parameters. Simulation and experiment were conducted for validation of results of the proposed strategy.

According to the literature survey, the peg-in-hole problem, as well as the block and palm case study, have been employed by different researchers for evaluating their mathematical models on jamming prediction in different applications. Workpieces with circular cross-section are widely used in micro and macro-scale systems as far as positioning the shafts with V-type locators, pick and place micro-scale cells in the surgical operations, positioning the parts with a circular cross-section in the production lines using two-contact mechanisms, pick and position of the eye lenses in the eye surgery operations and so on. Despite the mentioned applications of the circular workpieces, no specific research has been published for investigating the jamming of the circular workpiece during its positioning or grasping in the fixture design or manipulation tasks. So, the main contribution of the present paper is to suggest a novel study to investigate the jamming phenomenon in the positioning of a circular workpiece on the horizontal surface. In this study, theoretical and numerical analyses are proposed for modeling and prediction of jamming occurrence in such configuration and their results are compared to each other. The proposed theoretical model can be used to calculate the most stable conditions for the V-type locators based on the specific coefficient of friction between the circular workpiece and locator and the direction and intensity of the external forces. The suggested model can be incorporated as a case study in further research to evaluate the suggested theoretical models in the prediction of the jamming phenomenon.

## 3. THEORETICAL FOUNDATION

Theoretical analysis is established based on two methods: force analysis and the minimum norm principle. Force analysis is performed based on the static equilibrium equations. The minimum norm principle is also employed to model the jamming occurrence by solving the corresponding optimization problem. Fig. 1 represents the configuration of the model. It consists of a circular workpiece that is going to be positioned on the horizontal surface. A hand (or palm) having rotational motion pushes the workpiece to move along the X-direction. The palm and the horizontal bar are joined together at the revolute joint. A global coordinate system (*X* - *Y*) is defined at the revolute joint. Also, two local coordinate systems (*n*-*t*) are located at the contact point between the workpiece and the horizontal surface (point A in Fig. 1) and workpiece and palm (point B in Fig. 1). A circular workpiece with radius r and center of mass (C.G.) is pushed forward by the force $F$ to travel along the horizontal surface until it is immobilized due to the jamming.

It is assumed that two frictional contacts (with the coefficient of friction denoted by $\mu$) are established between the circular workpiece, base surface, and palm at points A and B, respectively. By application of the angular velocity to the palm at the revolute joint, the force F pushes the circular workpiece to move along X-axis. Jamming occurs at a specific distance denoted by $x_{jam}$ and its corresponding palm angle denoted by $\theta_{jam}$. In the rest of the paper, these two parameters are going to be named as the jamming-in travel and jamming-in angle of the workpiece, respectively. By considering the mentioned assumptions, mathematical models are going to be studied in the next two sections.

### 3.1. Mathematical model: force analysis

Force analysis is initiated by adaptation of the equilibrium equations to the configuration of the problem that is represented in Fig. 1. Jamming occurs for the workpiece by changing the contact condition from sliding to the rolling mode at the contact point between the workpiece and the base surface (point A in Fig. 1). Since the palm applies continuous force to the workpiece and makes the workpiece move along the X-direction, the sliding condition should be established at the contact point between the palm and the workpiece (point B in Fig. 1). So, external force F is actually applied at the edge of the friction cone with angle $\alpha = \tan^{-1}(\mu)$. Mass of the block is denoted by m. The gravitational force $mg$ is applied to the workpiece at its center of geometry. By adaptation of the equilibrium equations for this configuration, reaction forces at the contact point A can be obtained as Eq. (1) in the global coordinate system $X$ - $Y$:

$$\begin{aligned} R_t &= F_n \sin(\theta) - F_t \cos(\theta) \\ R_n &= F_t \sin(\theta) - F_n \cos(\theta) + mg \end{aligned} \tag{1}$$

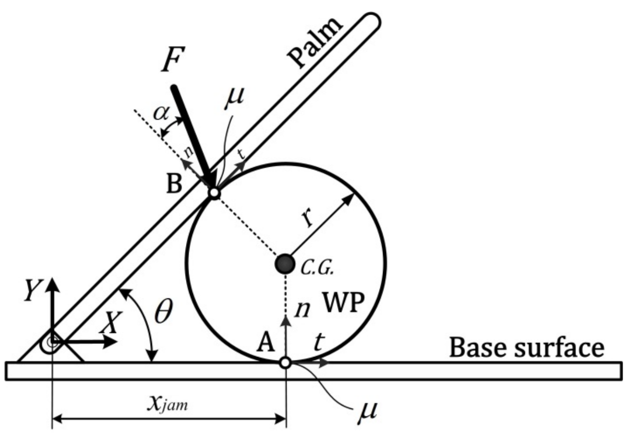


**Fig. 1. Configuration of the jamming model**

where, $R_t$ and $R_n$ stand for the normal and tangential components of the reaction force at point A. Similarly, $F_n$ and $F_t$ are the normal and tangential components of the external force $F$ at point B. These components can be obtained as $F\cos(\alpha)$ and $F\sin(\alpha)$, respectively. Jamming will occur for the circular workpiece if inequality $R_t < \mu R_n$ is satisfied at the specific value of the palm's angle of rotation $\theta_{jam}$. The jamming-in travel ( $x_{jam}$ ) can then be obtained as follows:

$$x_{jam} = \frac{r(1+\cos(\theta_{jam}))}{\tan(\theta_{jam})} + r\sin(\theta_{jam}) \tag{2}$$

By application of the external force $F$ to the workpiece at point A and assuming that the coefficient of friction is equal to $\mu$ at all of the contact points, the workpiece (with unit mass) starts to travel along X-direction until jamming occurs at the angle $\theta_{jam}$. Effects of the influence parameters on the jamming-in travel of the workpiece are also studied.

### 3.2. Mathematical model: minimum norm principle

Analytical modeling of the fixture is established based on applying the static equilibrium equations between the internal and external forces. Theoretical calculation of the reaction forces at the contact points is impossible in fixturing the 3D workpiece inside the typical 3-2-1 locating system. In such a fixturing system, 18 unknown reaction forces should be calculated while only six equilibrium equations are available for the fixture designer. The finite element method may be chosen as the first solution to this problem; however, incorporation of this tool has several shortcomings such as the lack of knowledge about the contact behavior between the workpiece and locators especially at the early stages of the fixture design process, the dependency of the results to the contact conditions, and extensive volume of calculation required for obtaining the results. The minimum norm principle acts as an efficient tool in the rapid calculation of the reaction forces at the contact points. It states that, in the statically indeterministic conditions, between all of the alternative answers to the static equilibrium equations, one with the minimum magnitude is the desired solution. Mathematical implementation of this principle can be described as a quadratic optimization problem, as follows:

Objective function:

$$\phi = \text{norm}(RF)$$
$$RF = (RF_n, RF_t)$$

Constraints: (3)

$$T\phi + W_e = 0$$
$$(RF_n) > 0$$
$$|RF_t| < \mu(|RF_n|)$$

where, $\phi$ is the norm of the reaction force vector $RF$ which has two components $RF_n, RF_t$ in the normal and tangential directions. The design variable of the optimization problem is the magnitude of the resultant reaction force vector. Hence, the parameter that should be minimized can be described as Eq. (4).

$$\phi = \sqrt{RF_n^2 + RF_t^2} \Rightarrow \phi^2 = RF_n^2 + RF_t^2 \tag{4}$$

Reaction force components should be obtained in the local $n-t$ coordinate system. The local coordinate system is defined at the contact point between the circular workpiece and the horizontal surface (Fig. 1). Since the optimization problem is conFigured to calculate the reaction forces at the global $X-Y$ coordinate system (which is defined on the center point of the support in Fig. 1), reaction forces should be transformed from the local coordinate system to the global one. By using the transformation matrix $T$ , this transformation is performed. The transformation matrix $T$ can be calculated as follows:

$$T = [T_n \quad T_t] = \begin{bmatrix} n & t \\ r\times n & r\times t \end{bmatrix} = \begin{bmatrix} n_x & t_x \\ n_y & t_y \\ n_z & t_z \\ (r\times n)_x & (r\times t)_x \\ (r\times n)_y & (r\times t)_y \\ (r\times n)_z & (r\times t)_z \end{bmatrix} \tag{5}$$

where, $T_n$ and $T_l$ are components of the transformation matrix in the normal and tangential directions, respectively. Similarly, $n$ and $t$ stand for the normal and tangential unit vectors at the contact point A in Fig. 1. $r$ is the position vector of the contact point A in the global coordinate system. Subscripts $x, y$ , and $z$ are components of their corresponding vectors in the global *X, Y,* and *Z* directions, respectively. $W_e$ is the resultant external wrench vector which consists of the workpiece weight and loading or positioning forces. A wrench can be defined as a vector that contains six elements, three for the force vector and the rest three for the moment components. $W_e$ can be described as follows:

$$W_e = W_c + W_g$$
$$W_e = [F_c, r_c \times F_c] + [F_g, r_g \times F_g] \tag{6}$$

In which, $W_c$ and $W_g$ are wrenches corresponding to the clamping and the weight-induced forces and moments. $F_c$ is the clamping force vector and $r_c$ is the position vector of the clamping point. Similarly, $F_g$ is the weight-induces force vector and $r_g$ is the position vector of the point corresponding to the workpiece's center of geometry.

The first constraint of Eq. (3) is equivalent to the static equilibrium equation in the global coordinate system. The second one states that the contact should be kept between the workpiece and the horizontal surface during its positioning or loading process. The third constraint stands for the Coulomb's friction law in the 2D workspace. Jamming would occur for the workpiece if a feasible solution is found for this optimization problem. In such a condition, all of the constraints are satisfied and no sliding is observed at the contact point between the circular workpiece and the horizontal surface. By the occurrence of jamming in the mentioned configuration, the jamming-in angle $\theta_{jam}$ and its corresponding jamming-in travel of the workpiece $x_{jam}$ are determined and compared to the predictions of the first theory and the numerical results.

The optimization problem is solved using the *fmincon* function and its utilities in MATLAB software. This solver provides several algorithms for solving the optimization problem namely interior-point, *active-set*, *sqp* and *trust-region-reflective* models. Based on the MATLAB recommendation on the selection of the appropriate algorithm, the proposed optimization problem is solved using the first three mentioned algorithms. The same results are obtained for the problem by the incorporation of these algorithms. Since the dimensions of the optimization problem are low (equal to 2 in the mentioned optimization problem), a feasible solution for the optimization problem is usually found out with just a few iterations. Hence, the problem is converged to a feasible solution with a high convergence rate. A typical graph of the convergence rate will be presented in section 5.

## 4. NUMERICAL ANALYSIS

Numerical analysis of the workpiece jamming is conducted using Adams® (ver. 2016) software. The model of the case study is represented in Fig. 2. For the numerical analysis, a circular workpiece with unit mass was designed with a radius equal to 10mm. The base surface and the palm were modeled by using two bars with rectangular cross-sections. The base surface was modeled using a box with dimensions $150\text{mm}\times 1\text{mm}\times 5\text{mm}$. It was defined as the ground part of the model. Palm was modeled using a rounded rectangle with the same dimensions. A revolute joint was located at the junction point between the palm and the base surface to accommodate the rotational motion of the palm with respect to the ground. A translational joint was located between the circular workpiece and the base surface by taking into account the static and dynamic coefficients of friction values. Stiction transition velocity was set to 0.1mm/s. By application of the angular velocity to the palm with the appropriate intensity, the velocity of the workpiece was increased enough to go beyond this value, immediately. So, it was ensured that the contact between the workpiece and the base surface was established with the dynamic coefficient of friction. It should be mentioned that the effects of the coefficient of friction were also studied on the jamming-in travel of the workpiece. As an initial study, it was assumed that the circular workpiece had only sliding movement along the *X*-direction and the rolling motion of the workpiece was assumed to be negligible.

Solid to solid contact was defined between the palm and the circular workpiece with the same values of static and dynamic coefficients of friction. Contact parameters were set according to the configuration of the problem and suggestions that were proposed in references [18, 19]. Contact

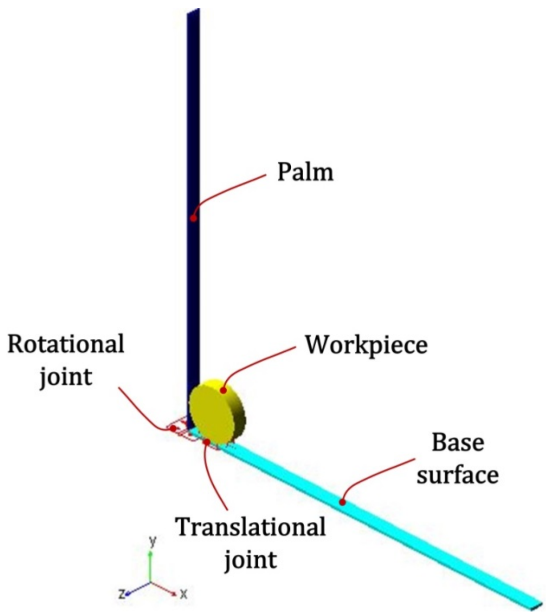


**Fig. 2. Model of the circle-palm case study in Adams® software**

stiffness, force exponent, damping ratio, and penetration depth were assumed to be equal to $1\times10^{8}$, $2.2$, $1\times10^{5}$ and $1\times10^{-2}$, respectively. Stiction transition velocity and friction transition velocity were also set to $0.1\text{mm}/\text{s}$ and $0.2\text{mm}/\text{s}$, respectively. It should be mentioned that the coefficient of friction increases from zero to $\mu_s$ by increasing the contact velocity from zero to the stiction transition velocity $(V_s)$. By a further increase in the contact velocity from $V_s$ to $V_d$ (friction transition velocity), the coefficient of friction decreases from $\mu_s$ to $\mu_d$. So, the constraint $V_s < V_d$ should be satisfied between the stiction and friction transition velocities. Usually, $V_s$ and $V_d$ takes small values to ensure that the contact is established with the dynamic coefficient of friction ($\mu_d = 0.4$ in the present study). For this purpose, the angular velocity of the palm was assumed to be equal to $30\text{deg}/\text{s}$. Gravity acceleration was defined as equal to $9806\text{mm}/\text{s}^2$ in the −Y direction. By application of the mentioned assumptions and parameters to the configuration of Fig. 2, the model was solved using the dynamic simulation solver. Jamming-in travel of workpiece $(x_{jam})$ was obtained by considering different values of the input parameters.

## 5. RESULTS AND DISCUSSION

In this section, predictions of the proposed mathematical models are compared to the numerical results. Assumptions mentioned in section 3 were used in the mathematical models. Fig. 3 represents the results of the first mathematical model. It represents the theoretical predictions for jamming-in travel of the workpiece and its corresponding angle of rotation regards to the coefficient of friction. The whole space is divided into the jamming and non-jamming regions. If the coefficient of friction and angle of rotation coincide in the non-jamming region, it can be concluded that jamming would not occur for the workpiece on the base surface. The boundary edge

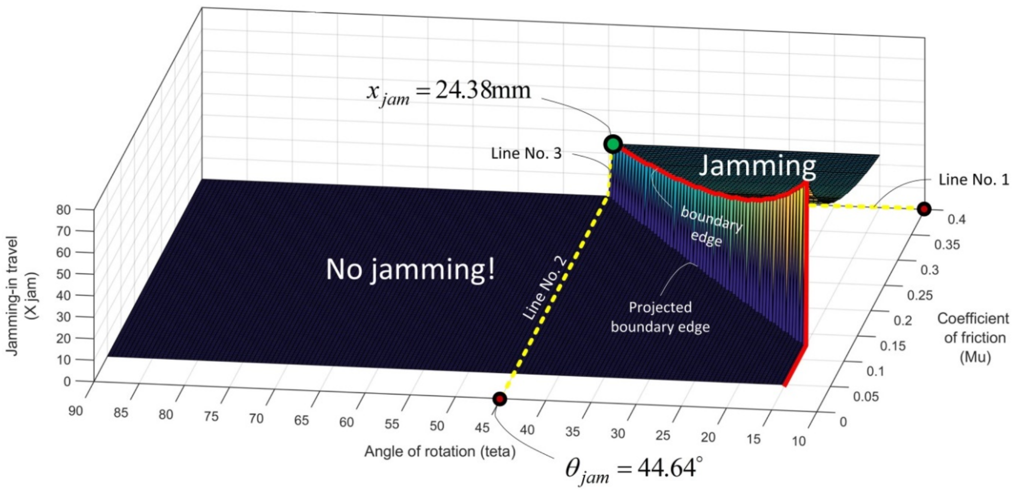


**Fig. 3. Contour plot of the jamming-in travel $(x_{jam})$ of the workpiece and its corresponding jamming-in angle $(\theta_{jam})$ regards to the coefficient of friction (obtained from the first theoretical model with assumptions $(m = 1\text{kg}, \mu = 0.4, r = 10\text{mm},$ and $F = 200\text{N})$**

separates two regions with a curve that represents the jamming initiation point for each value of the coefficient of friction. The following procedure should be used to take advantage of the contour plot. First, the coefficient of friction should be determined between the workpiece, palm, and base surface. A line (for example line No. 1 in Fig. 3) should then be drawn from the corresponding coefficient of friction in the first horizontal direction to intersect the projected boundary edge. By drawing line No. 2 in the second horizontal direction, the angle of rotation corresponding to the specified coefficient of friction can be determined. This angle is the jamming-in angle of the workpiece $(\theta_{jam})$. Finally, the third line (line No. 3) should be drawn in the vertical direction from the intersection point of these lines to the boundary edge to obtain the jamming-in travel of the workpiece $(x_{jam})$. For example, line No. 1 (corresponding to $\mu = 0.4$) has an intersection with line No. 2 (corresponding to $\theta_{jam} = 44.64^{\circ}$) on the projected boundary edge. By connecting this point to the boundary edge through line No. 3, jamming-in travel of workpiece can be obtained as $x_{jam} = 24.38\text{mm}$.

The second theoretical model was established based based on the minimum norm principle. It was coded in MATLAB software and solved using the quadratic optimization technique. Results were in accordance with the predictions of the first theoretical model. By taking into account the assumptions of the first theoretical model $(m = 1\text{kg}, \mu = 0.4, r = 10\text{mm},$ and $F = 200\text{N})$, transformation matrix and the resultant external wrench vector were obtained as follows for $\theta = 44.6^{\circ}$:

$$T = \begin{bmatrix} 0 & 1 \\ 1 & 0 \\ 0 & 0 \\ 0 & 0 \\ 0 & 0 \\ 27.38 & 0 \end{bmatrix}, \quad W_e = \begin{bmatrix} -77.5 \\ 194.2 \\ 0 \\ 0 \\ 0 \\ 476.7 \end{bmatrix} \tag{7}$$

By running the optimization problem, the normal and tangential components of the reaction force at the contact point were obtained as $RF_n = 194.2\text{N}$ and $RF_t = -77.5\text{N}$, respectively. It can be observed that the second and third constraints of Eq. (3) were satisfied with these values of the force components. By paying attention to the last rows of the transformation matrix and the external wrench vector in Eq. (7), another value can be obtained for the normal component of the reaction force as $RF_n = 17.41\text{N}$. This value of $RF_n$ was not acceptable because the third constraint was not satisfied with this value. Hence, jamming first occurred at the jamming-in angle $\theta_{jam} = 44.6^{\circ}$ and was maintained for the lower values of the palm's angle of rotation. By using Eq. (2), its equivalent jamming-in travel was obtained as $x_{jam} = 24.38\text{mm}$ which was equal to the first theoretical model. By increasing the palm's angle of rotation to $\theta = 44.7^{\circ}$, the third constraint of the optimization problem was violated. Also, the tangential component of the reaction force was decreased and remained below the threshold value $(\mu \times RF_n)$ by decreasing the palm's angle of rotation. Table 1 indicates the comparison between the predictions of the first and second theoretical models.

The maximum error equal to 0.6% was obtained for the jamming-in travel of the workpiece between the predictions of the suggested theoretical models. In the calculation of these error values, it was assumed that the predictions of the first theoretical model are accurate results; since it utilizes the direct (non-iterative) mathematical calculation of the jamming-in travel by using the static equilibrium equations. This amount of error is negligible for the second mathematical model. Running the optimization problem with different configurations, it was observed that the problem converges to feasible solutions with just a few iterations. So, the convergence rate is high because of the low dimensions of the optimization problem. Fig. 4 represents a typical convergence curve obtained from solving the optimization problem with the interior-point algorithm. It should be remembered that the objective function value is equal to $\phi^2$ where $\phi$ indicates

**Table 1. Comparison between the predictions of the first and second theoretical models on and**

| Coefficient of friction ($\mu$) | First theoretical model | | Second theoretical model | |
|---|---|---|---|---|
| | Jamming-in travel $x_{jam}$ [mm] | Jamming-in angle $\theta_{jam}$ [deg] | Jamming-in travel $x_{jam}$ [mm= | Jamming-in angle $\theta_{jam}$ [deg] |
| 0.45 | 21.64 | 49.6 | 21.53 | 49.8 |
| 0.4 | 24.38 | 44.6 | 24.26 | 44.8 |
| 0.35 | 27.85 | 39.5 | 27.78 | 39.6 |
| 0.3 | 35.50 | 34.2 | 35.50 | 34.2 |
| 0.25 | 39.09 | 28.7 | 39.23 | 28.6 |
| 0.2 | 48.93 | 23.1 | 48.93 | 23.1 |
| 0.15 | 65.35 | 17.4 | 65.73 | 17.3 |

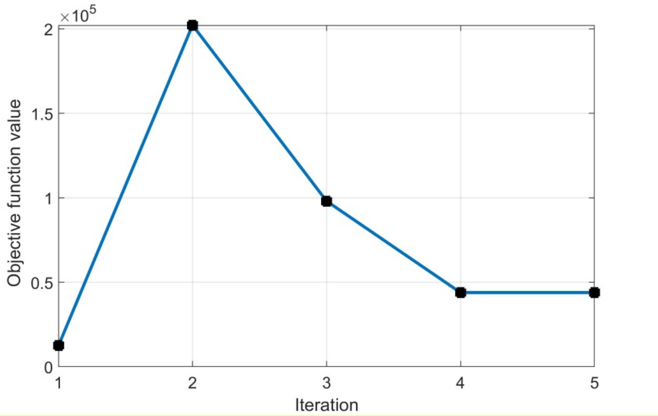


**Fig. 4. A typical convergence curve obtained from solving the optimization problem with the interior-point algorithm with assumptions** ($m = 1$kg, $\mu = 0.4$, $r = 10$mm, **and** $F = 200$N **)**

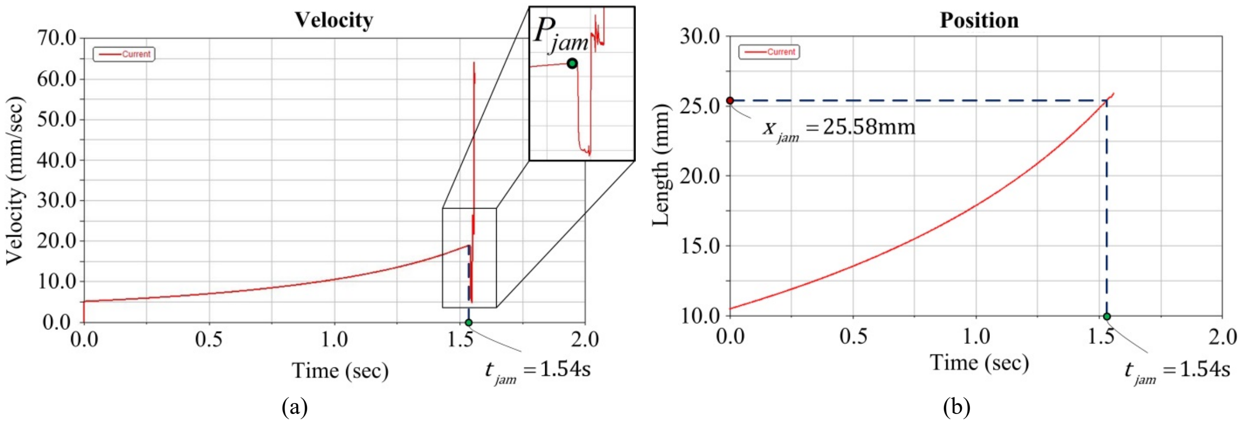


**Fig. 5. Results of the simulation: (a) velocity of the workpiece along *X* direction regards to the time, and (b) position curve of the block (with assumptions:** $m = 1$kg, $\mu = 0.4$, $r = 10$mm, $\omega$=30deg/s, **and** $g$=9.8m/s$^2$)

the magnitude of the resultant reaction force vector at the contact point. It can be observed that the problem rapidly converges to the final solution with just five iterations.

By comparing the predictions of the theoretical models, it can be concluded that the same predictions of the jamming-in travel and jamming-in angle of the workpiece can be obtained from both of the suggested theoretical models. This behavior was observed for different values of the coefficient of friction, radius of the workpiece, and intensity of the external wrenches.

Predictions of the theoretical models were validated

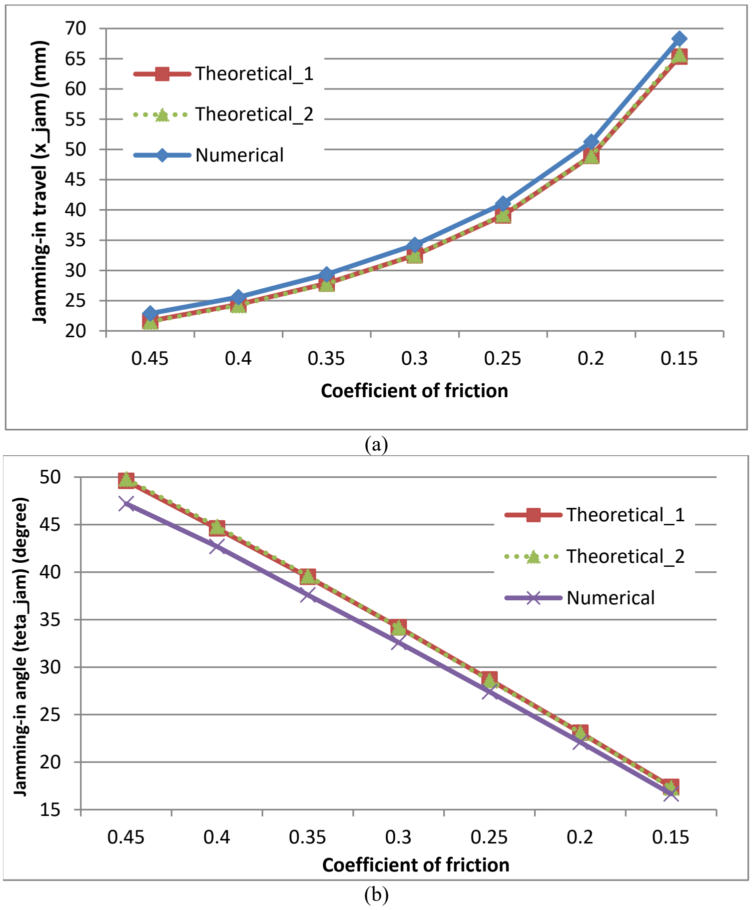


**Fig. 6. Comparison between the theoretical predictions and the numerical results with regards to the coefficient of friction, (a) jamming-in travel of workpiece, and (b) jamming-in angle of the workpiece (with assumptions:** $m=1\text{kg}, \mu=0.4, r=10\text{mm}, \omega=30\text{deg/s}$, **and** $g=9.8\text{m/s}^2$)

through numerical analysis. Before comparing the numerical results to the theoretical predictions, jamming occurrence should first be determined in the numerical results by investigating the kinematic parameters of the workpiece's motion. Fig. 5(a) represents a typical curve of the workpiece velocity which has been obtained with the assumption of $\mu_d=0.4$ at the contact points. Instability in the workpiece velocity can be observed in the jamming point $P_{jam}$ at the jamming time $t_{jam}$. It indicates the jamming occurrence in this configuration. Jamming-in travel of workpiece can be obtained by mapping this time on the vertical axis of the position curve (Fig. 5(b)). Hence, jamming-in travel of workpiece can be obtained as $x_{jam}=25.58\text{mm}$ from the numerical analysis. Since accurate results are achieved by the mathematical model, numerical results are compared to the theoretical ones. By assuming $\mu_d=0.4$, relative error equal to 4.9% is obtained in the prediction of the jamming-in travel of workpiece from the numerical analysis.

Fig. 6 represents the comparison between the theoretical predictions and the numerical results. In Fig. 6(a), jamming-in travel of workpiece is obtained with regards to the coefficient friction from the theoretical models and numerical analysis. Predictions of the theoretical models are well-matched to each other with the worst-case error equal to 0.6%. By assuming that the results obtained from the first theoretical model are accurate, the maximum error equal to 5.7% was obtained for $x_{jam}$ from the numerical analysis.

Fig. 6(b) represents the comparison between the theoretical predictions and numerical results on the jamming-in angle of the workpiece. A maximum error equal to 0.4% was obtained between the predictions of the theoretical models. Also, the theoretical predictions of the first model are well-matched to the numerical results with a maximum error value equal to 4.8%. The relatively small values of the errors in the numerical analysis represent the accuracy of the simulation and its results.

It can also be observed in Fig. 6(a) that the jamming-in travel of the workpiece is increased by decreasing the coefficient of friction. This phenomenon seems to be reasonable by paying attention to the geometry and configuration of the problem. In comparison to the high values of the coefficient of friction, the workpiece should travel more in the low values to jam and immobilize on the base surface.

The radius of the circular workpiece also affects its

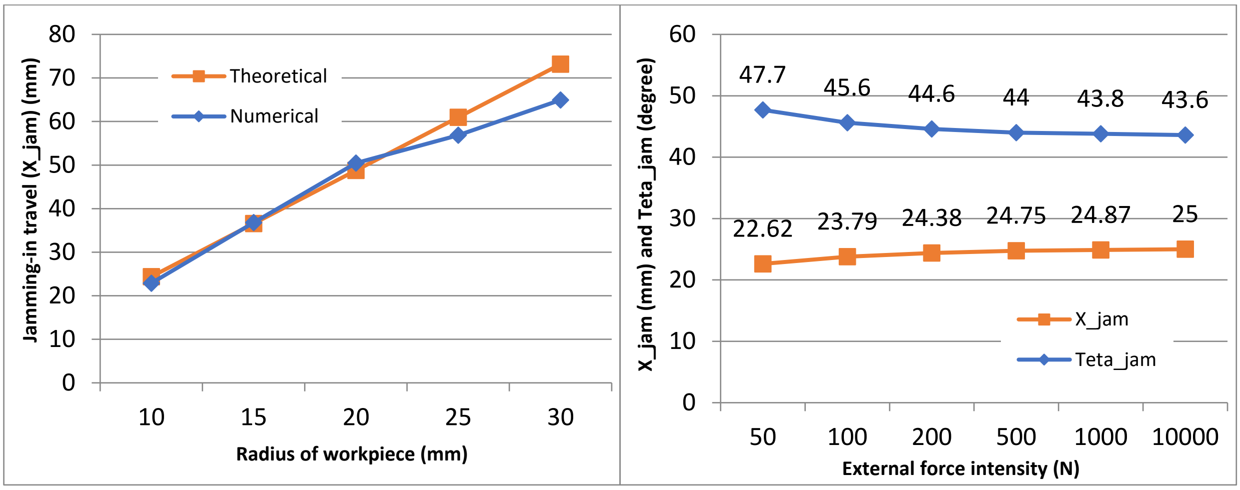


(a) (b)

**Fig. 7. (a) Effect of the radius of workpiece on the jamming-in travel, and (b) effect of the external force intensity on the jamming-in travel and jamming-in angle of the workpiece, which are obtained from the theoretical models**

jamming-in travel. Five levels were chosen for the radius of the workpiece including $r = 10, 15, 20, 25,$ and $30\text{mm}$. Fig. 7(a) represents the curves of $x_{jam}$ regard to the radius of the workpiece. It was assumed that the mass of the workpiece was remained constant through controlling its density. By this assumption, the net effect of the radius of the workpiece can be obtained on the $x_{jam}$. It can be observed that $x_{jam}$ has been increased by increasing the radius of the workpiece from both the theoretical model and the numerical analysis. The numerical results have been well matched to those of the theoretical model with the worst-case error value of 11.2%. An interesting result was observed for $\theta_{jam}$ where it remained almost constant for different values of the radius of the workpiece.

External force intensity may also be considered as one of the influence parameters in the theoretical models. Six levels were chosen for this parameter to study its effect on $x_{jam}$ including $|F| = 50, 100, 200, 1000,$ and $10000\text{N}$. The last level includes a force with extra high intensity. This level of force will be used for proving the fact that the external force intensity does not affect the jamming-in travel of the workpiece in the mentioned configuration. Fig. 7(b) represents the results obtained from the theoretical model. It can be observed that the jamming-in travel and jamming-in angle of the workpiece reached the threshold values by increasing the external force intensity. By applying the external force with the maximum intensity ($|F| = 10\text{kN}$), threshold values of $x_{jam}$ and $\theta_{jam}$ have been obtained as $25\text{mm}$ and $43.6°$, respectively. These values remained constant by the further increase in the external force intensity. Since the force intensity equal to 200N was incorporated in the present study, the relative error value equal to 2.29% was obtained for $x_{jam}$ in comparison with the case in which the external force was applied to the workpiece with the maximum intensity ($|F| = 10\text{kN}$). Although error values have been decreased by the increase in the external force intensity, it seems to be unreasonable to apply such forces to the workpiece in the mentioned configuration. By paying attention to the error values, it can be concluded that the effects of the external force intensity can be neglected on the jamming-in travel and jamming-in angle of the workpiece in the mentioned configuration. It was also observed that the mass of the workpiece did not affect the jamming-in travel and jamming-in angle of the workpiece in both the theoretical models and the numerical analysis. The same behavior was observed for the angular velocity of the palm in the simulation. It should be noted that the theoretical predictions and numerical results of the suggested models can't be compared to the previous data since no specific research has been published in the literature similar to the subject of the present paper.

## 6. CONCLUSIONS

In the present study, mathematical models were developed for the prediction of jamming of the circular workpiece during its positioning on the horizontal base surface. Two models were suggested for the mathematical foundation including the force analysis and the minimum norm principle. Numerical analysis was conducted using Adams software to validate the theoretical predictions. It was concluded that the suggested theoretical models predicted the workpiece jamming conditions with accepTable accuracy. With the mentioned assumptions, numerical results on the jamming-in travel of the workpiece were matched to the theoretical predictions with the error value equal to 4.92%. It was also concluded that the jamming-in travel of the workpiece was increased by decreasing values of the coefficient of friction in the interval [0.15-0.45]. By assuming that the workpiece mass is constant, it was shown that the jamming-in travel of the workpiece was increased by increasing the radius of the circular workpiece. By increasing the external force intensity, the jamming-in travel of the workpiece reached a threshold value. It remained constant by the further increase in the external force intensity. Mass of workpiece and angular velocity of palm had no sensible effect on the jamming-in travel of workpiece in the mentioned configuration.

For further study, experimental tests can be conducted for validating the theoretical predictions and numerical results. Consideration of the potential rolling motion of the workpiece in mathematical modeling and numerical analysis is also an active research field in this area.

## NOMENCLATURE

| | |
|---|---|
| $C.G.$ | *center of geometry of the workpiece* |
| $F$ | external positioning force |
| $F_c$ | resultant clamping force vector |
| $F_g$ | weight-induced force vector |
| $F_n, F_t$ | normal and tangential components of the external force |
| $g$ | gravitational acceleration |
| $m$ | mass of workpiece |
| $n$ | normal vector at the contact point |
| $n-t$ | local coordinate system |
| $P_{jam}$ | jamming point on the velocity curve |
| $RF$ | reaction force vector |
| $RF_n, RF_t$ | normal and tangential components of the reaction force vector |
| $R_n, R_t$ | normal and tangential components of the reaction force |
| $r$ | radius of the circular workpiece |
| $r_c$ | position vector of the clamping point |
| $r_g$ | position vector of the workpiece's center of geometry |
| $T$ | transformation matrix from local to global coordinate systems |
| $T_n, T_t$ | normal and tangential components of the transformation matrix $T$ |
| $t$ | tangential vector at the contact point |
| $V_d$ | *friction transition velocity* |
| $V_s$ | stiction transition velocity |
| $W_c$ | resultant clamping wrench vector |
| $W_g$ | weight-induced wrench vector |
| $W_e$ | resultant external wrench vector |
| $X-Y$ | global coordinate system |
| $x_{jam}$ | jamming-in travel of the workpiece |
| ***Greek symbols*** | |
| $\alpha$ | angle of the friction cone |
| $\omega$ | angular velocity of the palm |
| $\theta$ | angle of the palm |
| $\theta_{jam}$ | jamming-in angle of the workpiece |
| $\mu$ | coefficient of friction |
| $\phi$ | norm of the resultant reaction force vector |
| ***Subscript*** | |
| $n$ | normal direction |
| $t$ | tangential direction |
| $jam$ | jamming situation |
| $x, y, z$ | components of the corresponding vector at the global $X, Y$, and $Z$ directions |

## REFERENCES


[1] J.S. Pang, J.C. Trinkle, G. Lo, A complementarity approach to a quasistatic multi-rigid-body contact problem, Computational Optimization and Applications, 5(2) (1996) 139-154

[2] P.E. Dupont, S.P. Yamajako, Jamming and wedging in constrained rigid body dynamics, in: Proceeding of the IEEE International Conference on Robotics and Automation, San Diego, 1994, pp. 2349-2354

[3] J.C. Trinkle, D.C. Zeng, Prediction of the quasistatic planar motion of a contacted rigid body, IEEE Transactions on Robotics and Automation, 11(2) (1995) 229-246

[4] J.C. Trinkle, S.L. Yeap, L. Han, When quasistatic jamming is impossible, in: IEEE International Conference on Robotics and Automation, Minneapolis, MN, USA, 1996, pp. 3401-3406

[5] D.J. Balkcom, J.C. Trinkle, Computing wrench cones for planar rigid body contact tasks, International Journal of Robotics Research, 21(12) (2002) 1053-1066

[6] T. Liu, M.Y. Wang, Computation of three-dimensional rigid-body dynamics with multiple unilateral contacts using time-stepping and Gauss-Seidel methods, IEEE Transactions on Automation Science and Engineering, 2(1) (2005) 19-31

[7] T. Liu, M.Y. Wang, K.H. Low, Non-jamming conditions in multi-contact rigid-body dynamics, Multibody System Dynamics, 22(2) (2009) 269-295

[8] J. Bender, K. Erleben, J. Trinkle, Interactive simulation of rigid body dynamics in computer graphics, in: Computer Graphics Forum, 2014, pp. 246-270

[9] D.M. Flickinger, J. Williams, J.C. Trinkle, Performance of a method for formulating geometrically exact complementarity constraints in multibody dynamic simulation, Journal of Computational and Nonlinear Dynamics, 10(1) (2014) 1-12

[10] Y. Lu, J. Williams, J. Trinkle, C. Lacoursiere, A framework for problem standardization and algorithm comparison in multibody system, in: ASME International Design Engineering Technical Conferences and Computers and Information in Engineering Conference, Buffalo, New York, USA, 2015

[11] H. Parvaz, M.J. Nategh, Development of an efcient method of jamming prediction for designing locating systems in computer-aided fxture design, International Journal of Advanced Manufacturing Technology, 86(9-12) (2016) 2459-2471

[12] H. Parvaz, M.J. Nategh, Development of locating system design module for freeform workpieces in computer-aided fxture design platform, Computer Aided Design, 104(1) (2018) 1-14

[13] M.J. Nategh, H. Parvaz, Development of computer aided clamping system design for workpieces with freeform surfaces, Computer Aided Design, 95 (2018) 52-61

[14] K. Zhang, J. Xu, Force control for a rigid dual peg-in-hole assembly, Assembly Automation, 37(2) (2017) 200-207

[15] K. Zhang, J. Xu, H. Chen, J. Zhao, K. Chen, Jamming analysis and force control for flexible dual peg-in-hole assembly, IEEE Transactions on Industrial Elecetronics, 66(3) (2018) 1930-1939

[16] Y. Huang, X. Zhang, X. Chen, J. Ota, Vision-guided peg-in-hole assembly by Baxter robot, Advances in Mechanical Engineering, 9(12) (2017) 1-9

[17] Z. Hou, M. Philipp, K. Zhang, Y. Guan, K. Chen, J. Xu, Te learningbased optimization algorithm for robotic dual peg-in-hole assembly, Assembly Automation, 38(4) (2018) 369-375

[18] J. Giesbers, Contact Mechanics in ADMAS: A Technical evaluation of the contact models in multibody dynamics sofware MSC ADAMS, Bachelor thesis, University of Twente, Netherlands, 2012

[19] S. Frimpong, M. Tiruvengadam, Contact and joint forces modeling and simulation of crawler-formation interactions, Journal of Powder Metallurgy & Mining, 4(2) (2015) 135-149

**HOW TO CITE THIS ARTICLE**

*H. Parvaz. Theoretical and Numerical Analysis of Jamming Phenomenon in Positioning of Circular Workpiece on Horizontal Surface. AUT J. Mech Eng., 4(4) (2020) 553-564.*

**DOI:** 10.22060/ajme.2020.16132.5806